Int. J. Multiphase Flow Vol. 13, No. 3, pp. 357–364, 1987
Printed in Great Britain.

0301-9322/87 $3.00 + 0.00

EXPERIMENTAL STUDY OF THE FLOW PROPERTIES OF A HOMOGENEOUS SLURRY NEAR TRANSITIONAL REYNOLDS NUMBERS

M. A. ABBAS and C. T. CROWE
Department of Mechanical Engineering, Washington State University, Pullman, WA 99164-2920, U.S.A.

(*Received* 4 *May* 1986; *in revised form* 19 *September* 1986)

Abstract—The results of an experimental study on the pressure drop and velocity distribution of a homogeneous slurry flowing in a duct are reported. The slurry consisted of chloroform and silica gel with matched index of refraction to enable laser–Doppler measurements through the mixture. Slurries with two particle sizes at solids concentrations up to 30% were used. Velocity and pressure drop measurements were made in fully-developed flows with Reynolds numbers from 1200 to 30,000. The results show that the velocity distribution fits the logarithmic law of the wall with a modified Karman constant and turbulent boundary factor. The pressure drop measurements for the slurry with small particles (96 μm) indicate a transitional Reynolds number near that for a single-phase fluid. The corresponding measurements with large particles (210 μm) show no transitional effects over the Reynolds number range tested.

INTRODUCTION

The behavior of solid–liquid (slurry) flows in pipes has application to many engineering processes such as hydraulic conveying, transportation of food products and development of fuels using coal/water slurries. Previous analytical studies of a homogeneous slurry flow include the work of Zandi & Murthy (1969) and Hanks & Pratt (1967). These studies treat the slurry as a Bingham plastic or power law fluid and the relations for friction factors and velocity distribution are based on these models. However, there is little data available on the adequacy of these models or on the flow regimes for which they are valid. The early measurements of Daily & Hardison (1964) and Mih (1979), using impact probes, are subject to considerable doubt because particle–probe interference effects are large. Laser–Doppler anemometry (LDA) measurements made by Zisselmar & Molerus (1979) and Yianneskis & Whitelaw (1983) were limited to low solid concentrations. The purpose of this study was to investigate the pressure loss and velocity profiles of homogeneous slurries at concentrations, by volume, up to 30% and to establish the adequacy of rheological models for slurry flow properties.

EXPERIMENTAL APPARATUS AND PROCEDURE

A specific goal of this research was to measure the velocity distribution for a fully-developed homogeneous slurry. Because the Reynolds number was in the range of the transitional Reynolds number for single-phase flows, no intrusive measurement technique could be used. Based on the work of previous investigators, the LDA system, in conjunction with a solid–liquid mixture with matched index of refraction, was chosen.

The experiments were performed in the closed flow circuit depicted schematically in figure 1. A constant head reservoir was used to supply a steady flow. A propeller-type mixer was used to maintain uniform particle distribution. The velocity in the conveying pipe was regulated by means of a ball valve. The test section consisted of a pipe with an inside diameter of 17.5 mm. A glass tube was installed at the test section to facilitate LDA measurements. Piezometric tubes were installed at four stations along the pipe, 40 pipe diameters apart, to measure the pressure gradient along the pipe and calculate the friction factor. A constant pressure gradient, as measured by the piezometric tubes, indicated a fully-developed flow. Two other taps, 120 diameters apart, were connected to a pressure transducer to validate the pressure drop measurements. Special care was taken in the construction of the joints and taps to insure a smooth internal surface. A centrifugal

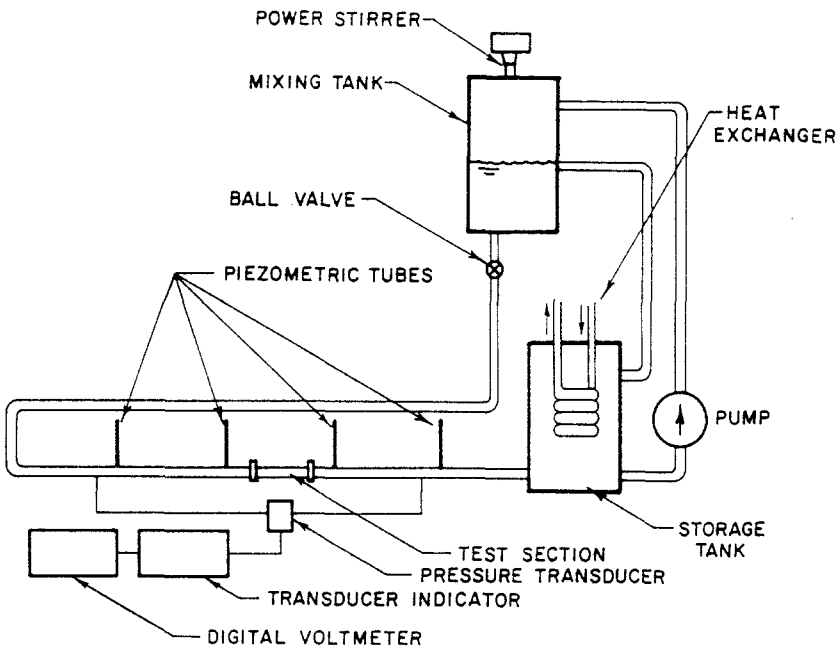

Figure 1. Schematic diagram of the slurry test loop.

pump returned the mixture to the constant head tank where a heat exchanger was used to maintain a constant mixture temperature.

After examining several solid–liquid mixtures, chloroform and silica gel were selected because measurements indicated that the difference in the refractive indices is of the order of 0.0001 at 20°C. Chloroform is available, reasonably priced, nontoxic, nonflammable, chemically stable, optically clear and colorless. However, it has some health hazards after extended exposure. The addition of water to the chloroform enabled a fine control on the chloroform's index of refraction. Specifically, the index of refraction was increased by 0.0004 by adding 0.0007 of water by volume to the chloroform. The silica gel was reagent-grade crystals. Two particle sizes were used. Measurement of the particle sizes using a Coulter counter indicated mass median diameters of 96 and 210 μm. The chloroform neither reacts with or is absorbed by the silica gel. The very minute volume fraction of water added to modify the index of refraction would not significantly alter the size of the silica gel particles if absorbed completely by the silica gel.

The LDA requires the presence of seeded particles as light scatters. In that sense, the LDA technique is well-suited to solid–liquid flows which include particles naturally. The refractive index of the silica gel was matched close enough to that of chloroform to enable LDA measurements without blockage of the laser beam. However, the difference in the refractive index was adequate to scatter sufficient light for velocity measurements.

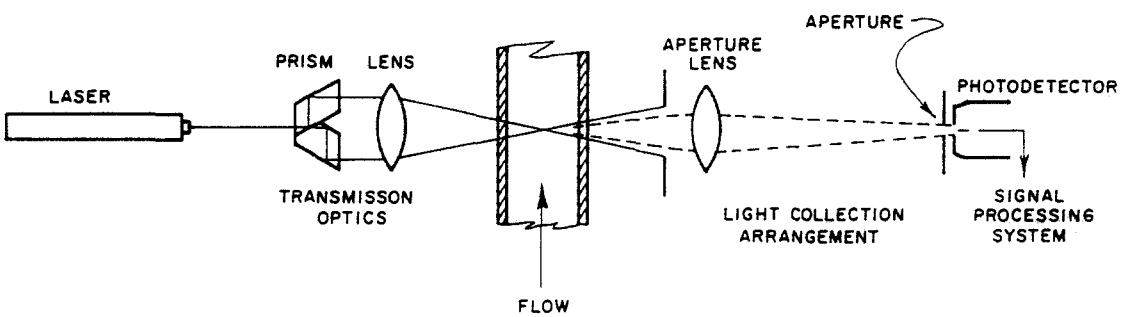

Figure 2. Laser–Doppler system.

The LDA optical system employed in the present study is shown schematically in figure 2. It consisted of a 5 mW He–Ne laser, an optical unit, receiving optics assembly, photodiode and a counter processor. The LDA system operated in the dual-beam, forward-scattering, fringe mode. The system was mounted on a traversing mechanism so that the LDA measuring volume could be moved across the pipe diameter in the horizontal plane. The mechanism was capable of positioning the optical system to within 0.025 mm. The positions of the slide mechanism were controlled by a micrometric screw and indicated by a dial indicator.

The LDA signals generated by a solid–liquid flow differ in amplitude depending on whether they originate from small particles in the chloroform as received or from the larger particles (silica gel) added to the fluid. The intensity of the light scattered from the large particles is higher than that from the small particles.

The signal processing system is shown in figure 3. The threshold level on the storage oscilloscope was set to trigger on signals from the silica gel particles which, in turn, enabled the counter processor to accept the data. The counter processor displayed the Doppler frequency, total number of fringes crossed for each burst and the time between two consecutive bursts. Silica gel particles which passed through the edge of the measuring volume and produced a signal smaller than the threshold level were not counted. The exclusion of these particles did not affect the local velocity measurements. The information from the counter processor was transferred to the S-100 microcomputer using the approach described by Stock & Lentz (1981). The output from the microcomputer was the weighted mean velocity and the standard deviation. Following Buchhave (1979), the mean velocity was calculated as follows:

$$U = \frac{\sum_{j=1}^{N} u_j W_j}{\sum_{j=1}^{N} W_j} \qquad [1]$$

where W_j is the residence time weighting factor and u_j is an individual velocity realization.

Velocity measurements were made along the pipe diameter in the horizontal plane. The measurements were started at one wall and made progressively toward the other wall. The position of the measuring volume was established using the inside pipe wall as a reference point.

In order to verify that the experimental apparatus was operating satisfactorily, preliminary experimental measurements were conducted using water. Velocity profiles, pressure drop and turbulence quantities were measured and compared to the well-established data for pipe flow. Agreement with these data indicated satisfactory operation of the system.

The mean flow velocity was determined by first integrating the local velocity measurements to obtain the discharge and then dividing by the pipe area. The discharge calculations were

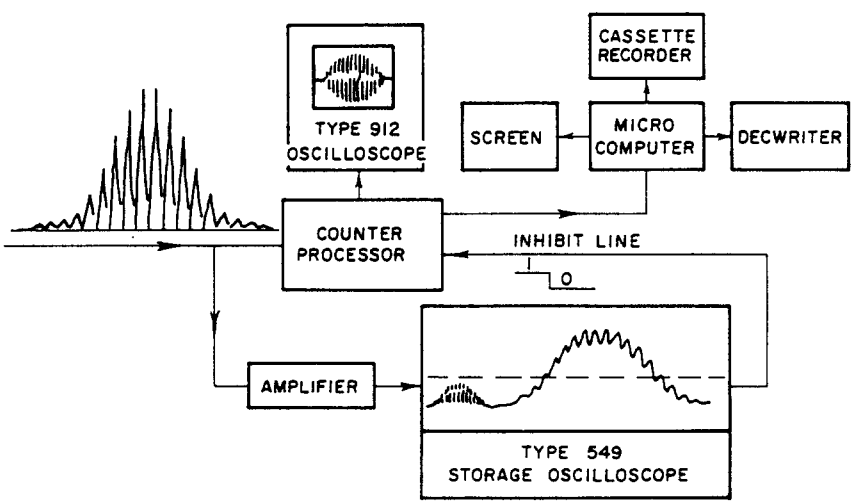

Figure 3. Signal-processing system.

corroborated by direct volume measurements of the discharge. The average wall shear stress τ_w was calculated directly from the pressure measurements:

$$\tau_w = \left(\frac{D}{4}\right)\left(\frac{\Delta P}{\Delta L}\right) \quad [2]$$

where $\Delta P/\Delta L$ is the negative pressure gradient and D is the pipe diameter. The Darcy–Weisbach friction factor was evaluated using

$$f = 8\frac{\tau_w}{\rho_L U^2}, \quad [3]$$

where U is the mean velocity and ρ_L is the density of the liquid phase.

RESULTS AND DISCUSSION

The velocity profiles measured for the slurry with the 96 μm particles are shown in figure 4. One notes that the profiles corresponding to Reynolds numbers <2400 assume the parabolic profile characteristic of laminar flow. However, at Reynolds numbers in the range of 2×10^4 the profile assumes the blunt shape characteristic of turbulent pipe flow.

The velocity profiles measured with the 210 μm particles are shown in figure 5. In this case, the profiles maintain a blunt, turbulent-like profile over the entire Reynolds number range.

The velocity profile for the fully-developed, turbulent flow of a single-phase fluid in a pipe can be fitted (except near the wall) with the law of the wall, namely

$$\frac{u}{u^*} = \frac{1}{K}\ln\left(\frac{yu^*}{\nu_L}\right) - \ln C, \quad \frac{yu^*}{\nu_L} < 500, \quad [4]$$

where

$$u^* = \left(\frac{\tau_w}{\rho_L}\right)^{\frac{1}{2}}$$

and K is the von Karman constant, y is the distance from the wall, u^* is the shear velocity and C is the turbulent boundary factor.

The velocity distribution data for the two slurries were also plotted on semilog coordinates corresponding to the law of the wall and the results are shown in figures 6 and 7. The measurements for chloroform alone agree closely with the law of the wall for a single-phase fluid. The slurry data display the same linear relationship with an increase in slope corresponding to a smaller von Karman constant and turbulent boundary factor. This indicates that the logarithmic law of velocity distribution is valid for flow of a homogeneous slurry with suitable modification of the von Karman constant. The velocity data for turbulent flow at other Reynolds numbers were plotted in the same

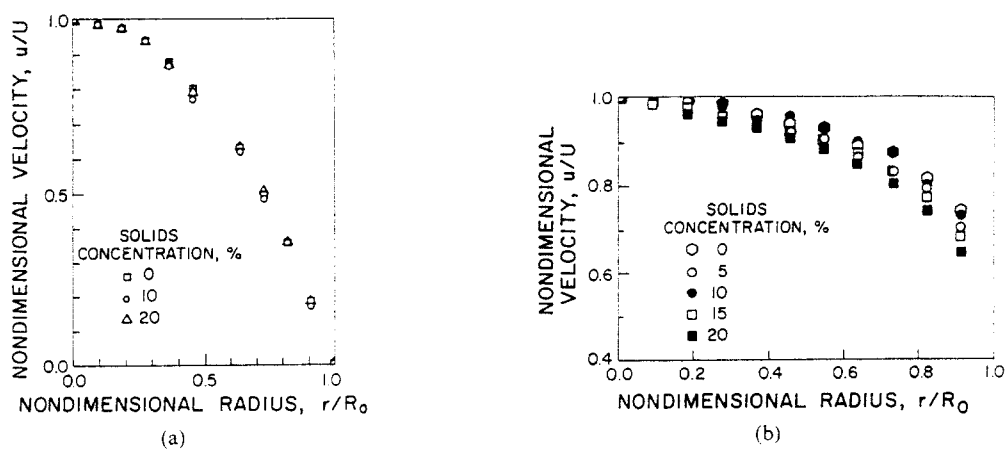

Figure 4. Radial velocity distribution for slurry with 96 μm particles for (a) Reynolds numbers in the range 1200–2000 and (b) Reynolds numbers in the range 15,000–30,000.

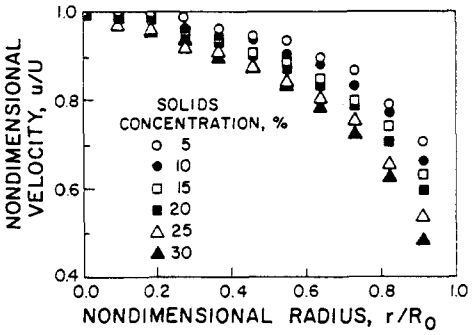

Figure 5. Radial velocity distribution for slurry with 210 μm particles at Reynolds numbers ranging from 1200 to 30,000.

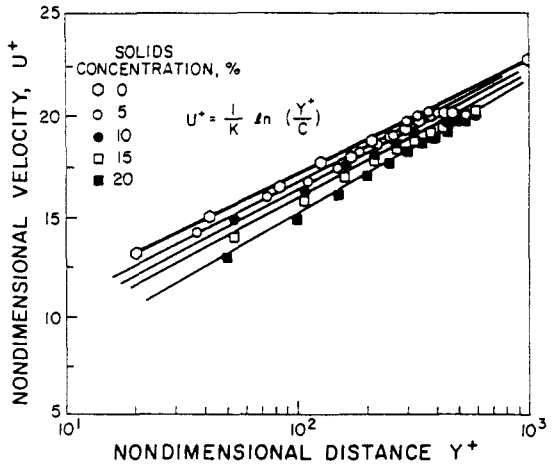

Figure 6. Nondimensional velocity distribution for slurry with 96 μm particles.

way. It was found that the von Karman constant was independent of Reynolds number and depended only on the solids concentration and particle size.

The observed logarithmic variation of velocity with radius indicates that neither the Bingham plastic nor power law rheological models are valid to represent the velocity profile in homogeneous slurry. In fact, the logarithmic profile suggests the flow model should be based on a turbulent mixing model analogous to Prandtl's mixing-length concept.

A plot of the von Karman constant vs the solid concentration for the two particle sizes is shown in figure 8. One notes a monotonic decrease in K with increasing concentration. Also, the decrease in K is more pronounced for the slurry with the 210 μm particles. Based on mixing-length theory, the decrease in K implies a reduced mixing length; i.e. the presence of the particles may impede the motion of the turbulent eddies.

The turbulent boundary factor, C, increases as the solid concentration increases as shown in figure 9. One also notes that C is affected by the particle size; C is larger for the slurry with the 210 μm particles.

The pressure drop measurement, together with the mean velocity as obtained by integration of the velocity distribution in the pipe was used to calculate the friction factor. The friction factor data were plotted vs Reynolds number based on the viscosity of the suspending fluid (chloroform). The friction factor–Reynolds number curves for the slurry with the 96 μm particles are shown in figure 10 for concentrations from 0 to 20%. The curve corresponding to pure chloroform agrees well with the standard curve for a smooth pipe. The curve also shows a discontinuity in the friction

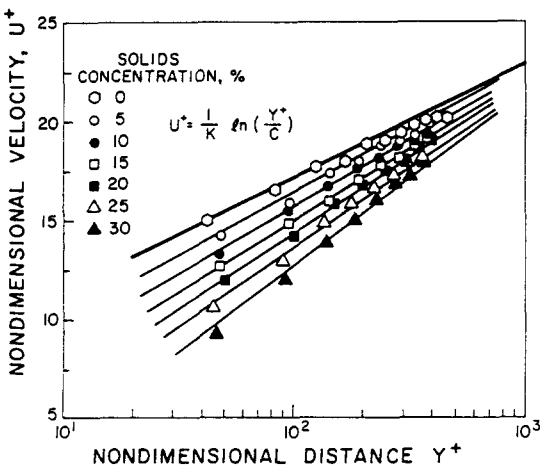

Figure 7. Nondimenstional velocity distribution for slurry with 210 μm particles.

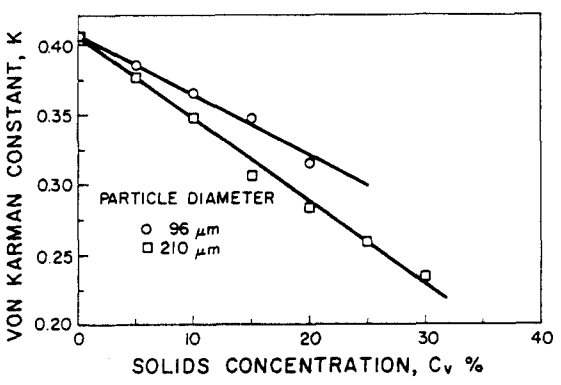

Figure 8. Von Karman constant vs solids concentration for slurries with two particle sizes.

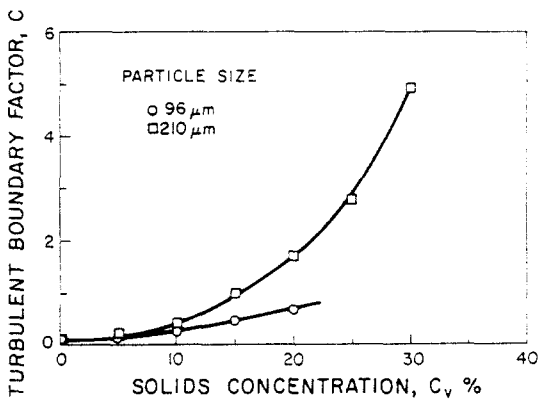

Figure 9. Turbulent boundary factor vs solids concentration for slurries with two particle sizes.

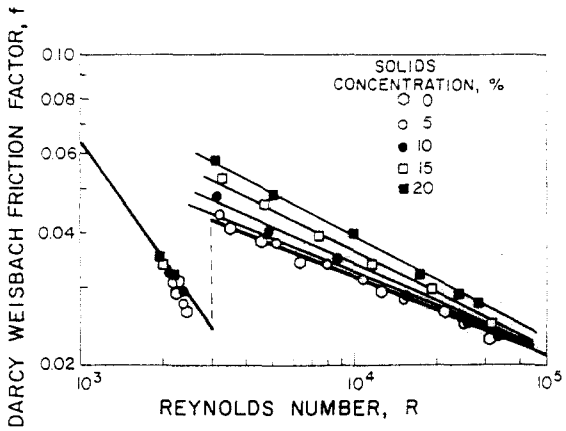

Figure 10. Friction factor vs Reynolds number for the slurry with the 96 μm particles.

factor at a Reynolds number near 3000 which is attributed to the transition from laminar to turbulent flow. The friction factor corresponding to turbulent flow increases with increasing solids concentration. However, the transitional effect continues to be apparent and the transitional Reynolds number is essentially unchanged. The concentration has no apparent effect on the friction factor in the subtransitional Reynolds number range.

The variation of friction factor with Reynolds number for the slurry with the 210 μm particles is shown in figure 11 for solids concentrations from 0 to 30%. The difference between figures 10 and 11 is significant. First, there is no apparent transition between laminar and turbulent flow for the 210 μm slurry as observed for the slurry with the 96 μm particles. Second, the friction factor is noticeably higher for the 210 μm slurry. Thus, particle size in a slurry is a critical parameter establishing the laminar or turbulent nature of the flow as well as the frictional pressure drop.

The relative turbulence intensities measured at the center of the pipe as a function of Reynolds number for the two slurries is shown in figure 12. The solids concentration of each slurry is 20%. The relative turbulence intensity in the slurries is slightly lower than that in a single-phase flow. At Reynolds numbers <3000, the relative turbulence intensity of the 96 μm particles was approx. 1%. At a Reynolds number of approx. 3000, the relative turbulent intensity jumps to approx. 3%. This same behavior was not evident for the slurry with the 210 μm particles as the relative turbulence intensity is essentially unchanged over the entire Reynolds number range. This implies no flow transitional effects over the Reynolds number range tested. These trends complement the observed transition in friction factor with Reynolds number for the two slurries.

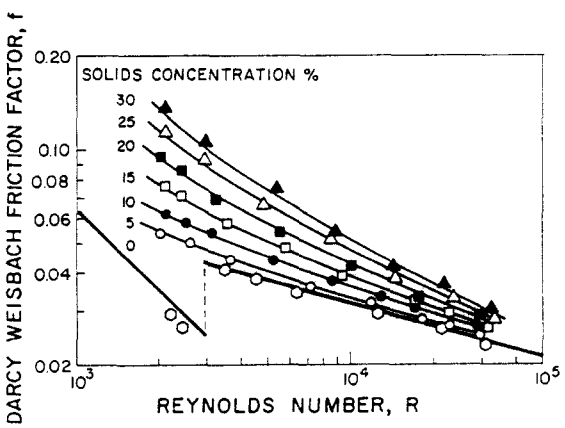

Figure 11. Friction factor vs Reynolds number for the slurry with the 210 μm particles.

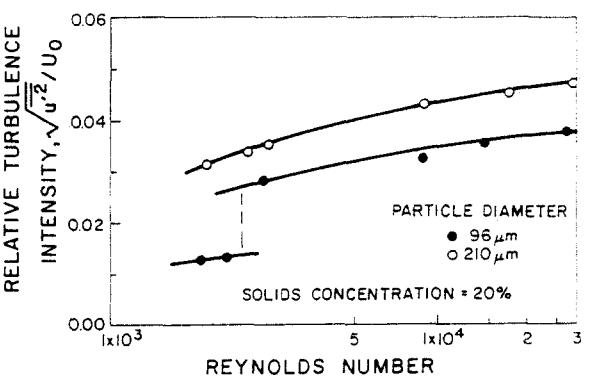

Figure 12. Relative turbulence intensity on the pipe centerline as a function of Reynolds number for slurries with two particle sizes at a solids concentration of 20%.

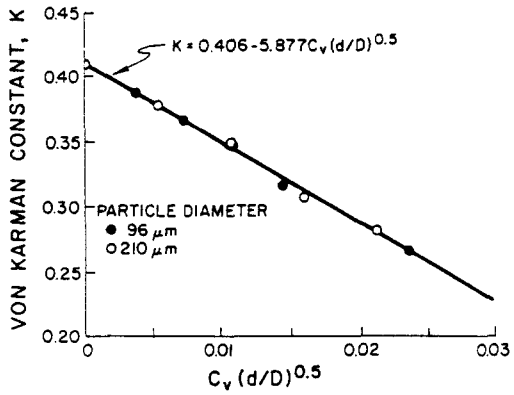

Figure 13. Von Karman constant vs the scaling parameter $C_v(d/D)^{1/2}$.

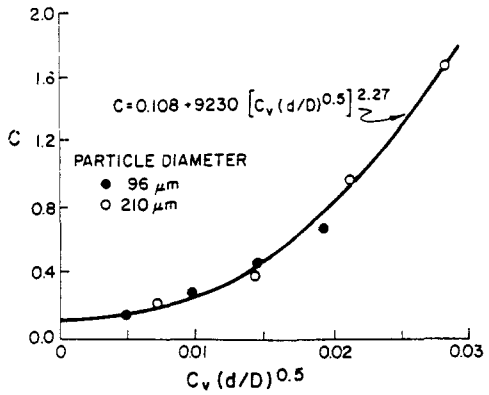

Figure 14. Turbulent boundary factor vs the scaling parameter $C_v(d/D)^{1.2}$.

Discussion of Data

In comparing the velocity profiles of the slurry with the universal law of the wall, one finds that the slurry data display the same linear relationship with an increase in slope (smaller von Karman constant). This suggests that the universal logarithmic law for velocity distribution is valid for the flow of a homogeneous slurry with suitable modification of the von Karman constant and turbulent boundary factor. This observation supports the theoretical development of Shen (1963). However, Shen predicted that K would increase with increasing solids concentration which is opposite to the trend observed in this study. The data show agreement with the trends observed by Mih (1979). However, the experimental results show that particle size affects the value of the von Karman constant, which was not observed by Mih.

Further study of the data for the von Karman constant show that the slope of the K vs C_v varies as the square root of the particle size. Thus, it was decided to fit the data with the linear function

$$K = K_0 - AC_v\left(\frac{d}{D}\right)^{0.5},$$

where K_0 is the Karman constant corresponding to the pure fluid, D is the pipe diameter and A is an empirical constant.

The data for the von Karman constant plotted as a function of $C_v(d/D)^{0.5}$ are shown in figure 13. One notes that the data for the two slurry particle sizes fall on a single curve demonstrating the suitability of $C_v(d/D)^{0.5}$ as a scaling parameter for the conditions of this study. The value of the empirical constant A is 5.9.

The fact that the von Karman constant K is dependent upon $C_v(d/D)^{0.5}$ suggests that the turbulent boundary factor C should depend also on the same parameter. It is proposed that C should be related to $C_v(d/D)^{0.5}$ by

$$C \propto \left[C_v\left(\frac{d}{D}\right)^{0.5}\right]^n.$$

Performing a nonlinear least-square curve fit on the experimental data relating C and $C_v(d/D)^{0.5}$, one obtains the expression

$$C = 0.11 + 9230\left[C_v\left(\frac{d}{D}\right)^{0.5}\right]^{2.27}.$$

A plot of the turbulent boundary factor vs $C_v(d/D)^{0.5}$ for the two slurry particle sizes is shown in figure 14. This figure also shows the suitability of $C_v(d/D)^{0.5}$ as a slurry parameter.

Conclusion

The velocity for a homogeneous slurry in a pipe varies logarithmically with the distance from the wall, corresponding to the universal law of the wall but with a modified von Karman constant

and turbulent boundary factor. The change in the von Karman constant and turbulent boundary factor depends on the product of the solids concentration (by volume) and the square root of the slurry particle diameter. Further data is needed to assess the effect of other parameters.

The particle size in the slurry influences the transition from laminar to turbulent flow. Small particles give rise to a transitional Reynolds number near that of a pure fluid. Larger particles appear to inhibit laminar flows and maintain a turbulent flow for Reynolds numbers as low as 1200.

The data also demonstrate the inadequacy of the Bingham plastic or power law rheological models for homogeneous slurries. The flow properties are established by the flow itself; i.e. by the turbulence. This suggests that the constitutive properties for the flow of a turbulent homogeneous slurry should be based on flow models rather than rheological models.

Acknowledgements—The support of the Mechanical Engineering Department, Washington State University, and the Government of Egypt is acknowledged. The authors are also appreciative of the assistance provided by Professor W. Mih (Civil Engineering Department) and Professor D. Stock (Mechanical Engineering Department).

REFERENCES

BUCHHAVE, P. 1979 The measurement of turbulent with the burst-type laser doppler anemometer—errors and corrections methods. Ph.D. Thesis, SUNY, Buffalo, N.Y.

DAILY, J. W. & HARDISON, R. W. 1964 Rigid particle suspension in turbulent shear flow. Technical Report No. 67, MIT Hydrodynamics Lab., Cambridge, Mass.

HANKS, R. W. & PRATT, D. R. 1967 On the flow of Bingham plastic slurries in pipes and between parallel plates. *Soc. Pet. Engrs* 342–346.

MIH, W. 1979 Transporting solid particles in smooth pipelines. *ASCE Trans. Engng J.* **105,** 427–437.

SHEN, C. C. 1963 Measurement of particle effects in flowing suspensions. M.S. Thesis, MIT, Cambridge, Mass.

STOCK, D. E. & LENTZ, R. A. 1981 Using S-100 based microcomputers in fluid mechanics laboratory. In *ASME/WAM Symp. on Computers in Flow Predictions and Fluid Dynamics Experiments*, pp. 229–236.

YIANNESKIS, M. & WHITELAW, J. H. 1983 Velocity characteristics of pipe and jet flows with high particle concentration. In *ASME Symp. on Liquid–Solid Flows and Erosion Wear in Industrial Equipment*, Vol. 13, pp. 12–15.

ZANDI, I. & MURTHY, V. R. 1969 Turbulent flow of non-Newtonian suspensions in pipes. *J. Engng Mech. Div. ASCE* **95,** (No. EMI), 271–288.

ZISSELMAR, R. & MOLERUS, O. 1979 Investigation of solid–liquid pipe flow with regard to turbulent modification. *Chem. Engng J.* **18,** 233–239.